ISIJ International, Vol. 47 (2007), No. 1, pp. 138–145

Pulsed Current GMAW for Superior Weld Quality of Austenitic Stainless Steel Sheet

Prakriti Kumar GHOSH, Shrirang Gurunath KULKARNI, Manish KUMAR and Harsh Kumar DHIMAN

Department of Metallurgical & Materials Engineering, Indian Institute of Technology Roorkee, Roorkee-247 667, Uttaranchal, India. E-mail: prakgfmt@rediffmail.com

(*Received on May 22, 2006; accepted on September 15, 2006*)

The performance of pulsed current gas metal arc welding (P-GMAW) and conventional gas metal arc welding (GMAW) processes in welding of 2.5 mm thin stainless steel sheet at different heat input has been studied. The use of P-GMAW at low heat input has been found superior to the use of GMAW process with respect to significant reduction in intergranular corrosion (IGC) susceptibility along with considerable improvement in some other characteristics of weld joint by maintaining comparable mechanical properties. It was further observed that the IGC, weld geometry and microstructure of P-GMA weld joint are largely governed by pulse parameters, and varies as a function of factor ϕ, defined as a summarized influence of pulse parameters such as peak current, base current, pulse-off time and pulse frequency. The increase of ϕ has been found favourable to reduce IGC, weld geometry along with refinement of the cast (dendritic) structure of weld deposit.

KEY WORDS: austenitic stainless steel; P-GMAW; inter granular corrosion; heat input; ϕ; weld geometry.

1. Introduction

Austenitic stainless steel sheets are largely used in many applications of automobile, chemical and food processing industries requiring good resistance to corrosion. Welding is largely used in fabrication of various components of this steel mostly by employing gas tungsten arc welding (GTAW) process. However, due to it's comparatively higher production rate and better compatibility to process automation the gas metal arc welding (GMAW) is often preferred by the industry over the GTAW.[1–3] But, the application of GMAW in sheet metal joining is quite critical due to difficulties in precise control of heat input. For sheet metal welding a low heat input is always preferred, where the use of pulsed current gas metal arc welding (P-GMAW) instead of the conventional gas metal arc welding (GMAW) may be more useful due to its ability to operate at low heat input in producing a sound weld.

During welding of austenitic stainless steel the formation of chromium carbide, especially in HAZ lying in the temperature range[4] of about 650–850°C, adversely affects the corrosion properties of the weld joint. The reduction in formation of chromium carbide requires welding at low heat input. The use of P-GMAW not only allows welding at comparatively low heat input but also provides further modification in thermal behaviour of weld joint by a control over the pulse parameters affecting the super heating of metal deposition.[5–10] However, the involvement of large number of simultaneously interactive pulse current parameters in P-GMAW, that includes pulsed current (I_p), base current (I_b), pulse time (t_p), pulse off time (t_b) and pulse frequency (f), introduces certain degree of complexity in controlling the process for desired welding.[5–10] It is reported with ample justification that the complexity of the process primarily arising due to criticality in selection of pulse parameters can be largely solved with the help of correlation of the weld characteristics with a summarized influence of pulse parameters defined by a dimensionless hypothetical factor $\phi=[(I_b/I_p)ft_b]$ derived from the energy balance concept of the process, where t_b is expressed as $[(1/f)-t_p]$.[8–10] In spite of its great potentialities hardly any systematic work has been reported so far on the joining of stainless steel sheet by controlled use of P-GMAW process in consideration of a summarized influence of pulse parameters.

In view of the above an investigation has been carried out to weld thin sheet of stainless steel at extra low heat input by employing P-GMAW with respect to that conveniently used in GMAW process. The superiority of using P-GMAW over P-GTAW in case of sheet metal welding has been analyzed at a low heat input where the latter has been found[3] to fail to produce consistent result with respect to weld geometry satisfying the DIN 8563 class AS standard. The control of weld thermal behaviour in P-GMAW has been further made by suitable modification of metal transfer through variation in pulse parameters. The weld joints have been characterized by studying the weld geometry, microstructure of weld deposit, behavior of HAZ and their mechanical properties.

2. Experimental

2.1. Welding

Square butt-welding of commercially available 2.5 mm thick austenitic stainless steel sheet has been carried out by

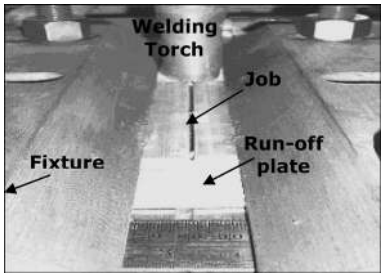

Fig. 1. Macro photograph showing joint set-up for preparation of weld joints.

Table 1. Chemical composition of the base material.

Material	Chemical composition (wt %)								
	C	Cr	Ni	Mn	Mo	Si	Cu	S	P
SS sheet	0.097	18.11	8.36	1.48	0.20	0.54	0.20	0.006	0.012
SS filler wire	0.022	19.65	9.55	1.25	0.10	0.39	0.08	0.007	0.016

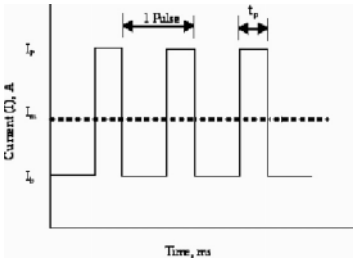

Fig. 2. Current waveform for pulsed current gas metal arc welding.

the GMAW and P-GMAW processes using a joint set-up as shown in **Fig. 1**. The welding was performed by semiautomatic process with the welding torch mounted on a carriage trolley having provision to regulate the travel speed. Both the welding processes were carried out under a gas shielding of commercial (99.98%) argon at a flow rate of 18 L/min and using 1.2 mm diameter 308L filler wire with direct current electrode positive (DCEP) at an electrode extension of 12 mm. During welding all the parameters were recorded with the help of transient recorder and WMS 4000 software installed in a computer connected to the circuit of the welding power source. The chemical compositions of the base metal and filler wire were analyzed under spark emission optical spectroscopy at a spot size of 3 mm on solid specimens as depicted in **Table 1**. The GMAW was carried out by lowering the heat input in steps of about 2 kJ/cm by varying the welding current and welding speed where the arc voltage was kept constant at 26 V. The heat input was lowered up to a value similar to that used by other workers[3] in P-GTA welding of thin SS sheets. For the P-GTA welding the heat input was estimated by assuming its arc voltage as 12 V which is lying within the usual range of the GTAW process as reported earlier.[11,12] The pulsed current welding, as it is schematically shown in **Fig. 2**, was performed at a low heat input with a variation in f from 0.12 to 0.41 to further favourably manipulate thermal behaviour[8–10] of the weld producing a sound joint. The low heat input of the P-GMAW process was decided in reference to the successfully tried lowest heat input of the conventional GMAW to produce flawless sound weld joint.

The welding parameters used in the GMAW and P-GMAW processes are shown in **Table 2** and **Table 3** respectively. Heat input of the GMA welding was estimated as follows whereas in case of the P-GMAW the heat input was estimated by using the mean current.

Table 2. Welding parameters and characteristics of GMA welds.

Heat input (kJ/cm)	Welding current (A)	Arc Voltage (V)	Welding Speed (cm/min.)	Dilution, D (%)	Estimated C (wt %)	Bead geometry, (mm)				Remarks
						b_1	b_2	a_1	a_2	
8.84	170	26	30.0	45.8	0.056	14.8	8.6	0.71	1.0	Full penetration
8.66	210	26	37.5	45.7	0.063	14.2	7.4	0.94	0.74	Full penetration
6.66	128	26	30.0	49.6	0.058	13.7	6.7	1.57	0.57	Full penetration
4.22	128	26	47.3	34.1	0.048	10.8	2.3	1.0	0.29	Full penetration

Table 3. Welding parameters and characteristics of P-GMA welds.

Heat input (kJ/cm)	ϕ	I_m (A)	I_p (A)	I_b (A)	f (Hz)	t_p (ms)	Arc Voltage (V)	Welding Speed (cm/min.)	Dilution D (%)	Estimated C (wt %)	Bead geometry (mm)				Remarks
											b_1	b_2	a_1	a_2	
4.44 ± 0.19	0.12	130	320	60	140	2.7	19.5	35.0	37.6	0.050	12	7.4	1.42	1.71	Full penetration
	0.23	131	260	80	100	2.7	21	35.0	39.5	0.052	10.4	6.7	1.57	1.28	Full penetration
	0.41	135	212	100	50	2.7	19.4	35.0	41.0	0.053	9.4	6.4	1.42	1.14	Full penetration

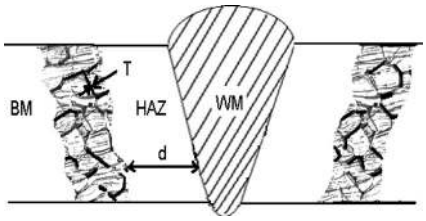

Fig. 3. Schematic characterization of sensitized zone with respect to its location, width and position from weld fusion line.

Heat input (J/cm)

$$= \frac{\text{Welding current (A)} \times \text{Arc voltage (V)}}{\text{Welding speed (cm/s)}} \quad \text{.....(1)}$$

2.2. Corrosion Studies

The transverse sections of the base material and weld joints were polished by standard metallographic procedure using diamond paste of 0.25 μm size particles. Inter granular corrosion test was carried out on the metallographic polished section of the base metal and weld joint by dipping them in the electrolytic solution of 100 g reagent grade oxalic acid ($H_2C_2O_4 \cdot 2H_2O$) in 900 mL distilled water using a current density of the order of 1 ± 0.1 A/cm^2 according to the specification ASTM A262. The susceptibility to IGC was studied in reference to the sensitization of HAZ defined by average grain boundary thickening (T) measured at different locations of HAZ starting from the region close to fusion line. After identifying a region showing severity of sensitization, its location in HAZ was also characterized (**Fig. 3**) by its average distance (d) from the weld fusion line measuring it at both sides of the weld joint. For a comparative understanding of the severity of grain boundary

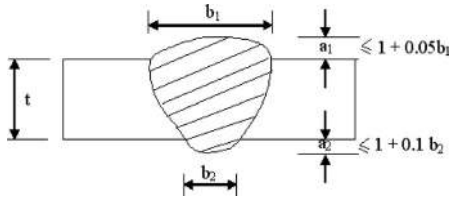

Fig. 4. Schematic diagram of weld bead profile as per DIN 8563 class AS.

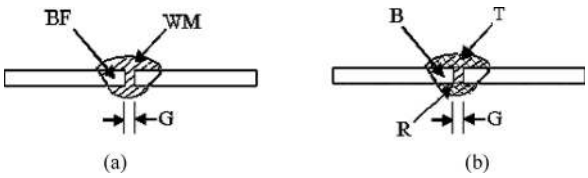

Fig. 5. Schematic diagram of graphical method used for estimating (a) weld deposit (WM), base metal fusion (BF) in consideration of the joint gap (G) used during welding and (b) areas of top (T) and root (R) reinforcements.

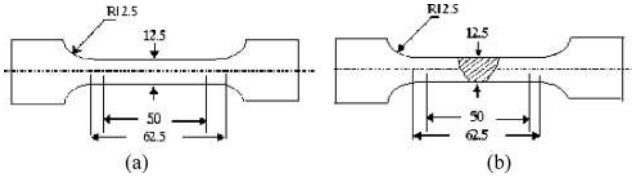

Fig. 6. Schematic diagram of tensile specimen used for testing of (a) base metal and (b) weld joints.

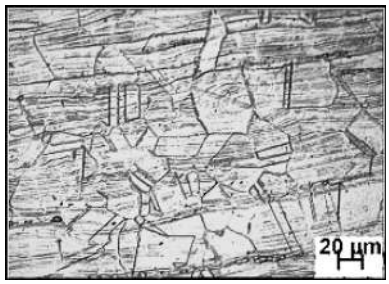

Fig. 7. Microstructure of base material.

thickening in HAZ the same measurement was also carried out in base material and in HAZ within 0.02 mm adjacent to fusion line along with sensitization of HAZ at a magnification of ×500 on at least 20–25 random locations with the help of the standard micro scale of image analysis facility available in the microscope. The microstructures of base metal and the sensitised region of HAZ of the weld joints prepared by GMAW and P-GMAW processes are also studied under scanning electron microscope (SEM) to reveal more clearly the morphology of grain boundary.

2.3. Studies on Weld Characteristics

The weld geometry, as it was clearly revealed by the etching in oxalic acid solution under IGC test, was also studied by optical microscopy. The weld geometry especially with respect to its top and root reinforcement (**Fig. 4**) was measured and compared as per DIN 8563 class AS standard to further justify the soundness of the weld joint. The area of weld joint (WJ) including the top and root reinforcements was measured by graphical method. The amount of weld metal deposition (WM), base metal fusion (BF) and dilution of weld deposit (D) were also estimated in terms of geometric solution of the graphic area, in consideration of the joint gap (G) used during welding (**Fig. 5**(a)) and estimated areas of the top (T) and root (R) reinforcements (Fig. 5(b)), as stated below.

$$WM\,(mm^2)=[T+G+R] \quad \text{.....(2)}$$

$$BF\,(mm^2)=[(T+G+R+2B)-(WM)] \quad \text{.....(3)}$$

$$WJ\,(mm^2)=[BF+WM] \quad \text{.....(4)}$$

$$D\,(\%)=[(BF/WJ)\times 100] \quad \text{.....(5)}$$

2.4. Microstructure Studies

The studies on microstructure under optical microscope were also carried on the IGC test specimens as it was clearly revealed by the etching in oxalic acid solution. The studies were carried out at the regions of different morphology primarily to compare the dendrite growth during solidification of weld deposit prepared by varying heat input and ϕ in the cases of GMAW and P-GMAW respectively.

2.5. Tensile Testing

Tensile testing of the base metal and axial weld joint having weld at its centre was carried out by using the flat tensile specimens as shown in **Figs. 6**(a) and 6(b), conforming the British Standard—B.S. 18: 1950. The tests were carried out at a crosshead speed of 1 mm/min. The tensile test was performed with the help of analytical software Q-Mat Dongle Version 3.83 and the yield strength was estimated at 0.2% offset strain.

3. Results and Discussion

3.1. Base Material

The chemical composition of base metal (Table 1) shows that it is not a stabilized grade stainless steel and hence it is significantly sensitive to the weld thermal cycle for precipitation of chromium carbide adversely affecting the properties of weld joint. Microstructure of the base material has been shown in **Fig. 7**. Figure 7 shows the typical microstructure of heavily rolled austenitic stainless steel sheet having twins in equiaxed grains along with considerable flow lines in the matrix. Thus, it may facilitate a thorough study concerning the influence of thermal behaviour on the characteristics of weld joint with respect to varying heat input and ϕ in the cases of GMAW and P-GMAW respectively. Besides heat input the variation in ϕ more precisely controls the thermal behaviour of weld joint through regulation of heat built up in weld pool due to its significant influence on energy distribution in the welding process dictated by the interactive pulse parameters[8–10,13]

3.2. Inter Granular Corrosion (IGC)

The effect of heat input on susceptibility of HAZ to IGC, characterised in terms of (Fig. 3) grain boundary thickening (T), and the distance (d) of the significantly sensitized region from the fusion line, in GMA weld joints has been

shown in **Table 4**. Similarly at a given heat input of 4.44 kJ/cm the effect of ϕ on susceptibility of HAZ to IGC in P-GMA weld joints has been shown in **Table 5**. Grain boundary thickening under the IGC test was also measured in base material for comparative study and was found as $0.82 \pm 0.16\ \mu$m. In weld joints it has been assumed that the grain boundary thickening is a function of IGC attack to the sensitised grain boundary which results from the precipitation of significant amount of chromium carbide within a specific range of temperature (650–850°C) prevailing for sufficient time.[4] Thus, more grain boundary thickening in comparison with that observed in base metal may be considered to be primarily attributed to larger sensitisation of HAZ. During welding the weld thermal cycle with respect to the heating rate, peak temperature and cooling rate of different location of HAZ in reference to fusion line varies significantly affecting its extent of sensitisation. In each weld joint (Tables 4 and 5) it is observed that the most sensitised region of HAZ, characterised by its comparatively larger grain boundary thickening than that of the HAZ close to the fusion line (FL), lies away from the FL and the *d* of this region also varies with the change in weld thermal behaviour dictated by the heat input and ϕ. The ϕ influencing the thermal behaviour of P-GMA weld has been reported earlier.[7–9] In case of GMAW it is observed (Table 4) that the decrease in heat input reduces the *d* and grain boundary thickening. The typical microphotographs depicting decrease in grain boundary thickening of the GMA weld joints with reduction of heat inputs from 8.84 to 4.22 kJ/cm have been shown in **Figs. 8**(a) and 8(b) respectively. The typical scanning electron micrograph of the base metal has been shown in **Fig. 9**. The scanning electron micrographs of the sensitized region of HAZ in GMA weld joints of different heat inputs of 4.22 and 8.84 kJ/cm have been shown in **Figs. 10**(a) and 10(b) respectively. The sensitized region of HAZ in P-GMA weld joint of low heat input of 4.22 kJ/cm as revealed under SEM has also been shown in **Fig. 11**. The SEM micrographs presented in Figs. 9–11 show that the revealing of grain boundary is possibly a function of degree of sensitization in this steel which is suppose to be lowest in the base metal as justified in Fig. 9. In agreement to this fact the micrographs presented in Figs. 10(a) and 10(b) clearly show that over all thickening of grain boundary in the sensitized region of GMA weld joint is relatively less at the lower heat input of 4.22 kJ/cm and it is further reduced in P-GMA weld joint (Fig. 11) of the similar low heat input. The SEM studies also reveal that the thickening of grain boundary may have primarily caused by

Table 4. Effect of heat input on inter granular corrosion of GMA weld joints.

Heat input (kJ/cm)		8.84	8.66	6.66	4.22
Grain boundary thickening near F.L.(μm ± σ)		1.27± 0.27	1.25± 0.32	1.19± 0.34	1.13 ± 0.21
Characteristics of the most sensitised region in HAZ	Distance from F.L., d (mm±σ)	5.58± 0.62	5.20± 0.05	4.92± 0.34	4.50± 0.15
	Grain boundary thickening, T (μm ± σ)	2.83± 0.75	2.61± 0.27	2.35± 0.67	2.28 ± 0.35

σ indicates standard deviation

Table 5. Effect of heat input and ϕ on inter granular corrosion of P-GMA weld joints.

Heat input (kJ/cm)		4.44 ± 0.19		
ϕ		0.12	0.23	0.41
Grain boundary thickening near F.L. (μm ± σ)		1.06± 0.20	0.99± 0.19	0.94± 0.28
Characteristics of the most sensitised region in HAZ	Distance from F.L. (mm±σ)	5.27± 0.12	5.18± 0.17	4.49± 0.23
	Grain boundary thickening (μm ± σ)	2.22± 0.58	2.05± 0.69	1.94± 0.47

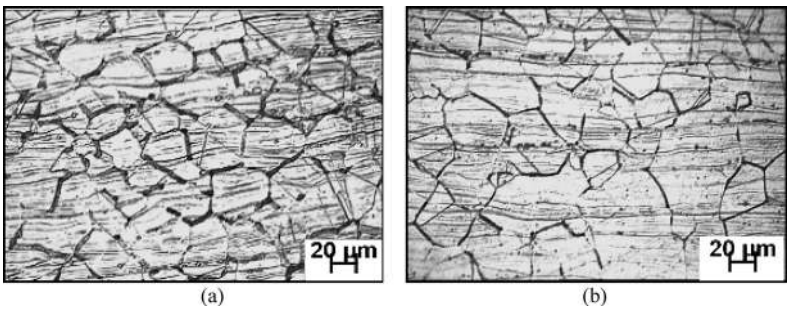

Fig. 8. Typical microphotograph showing IGC attack in HAZ of the GMAW at a heat input of (a) 8.84 kJ/cm and (b) 4.22 kJ/cm.

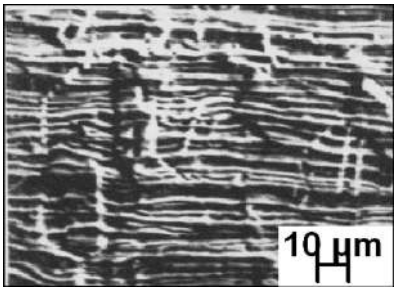

Fig. 9. Typical SEM micrograph of base metal.

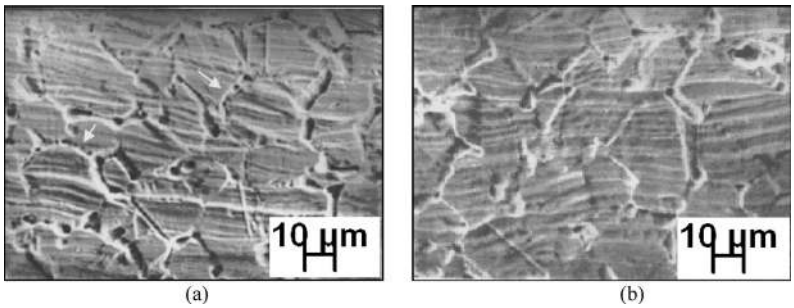

Fig. 10. Typical SEM micrograph showing IGC attack in HAZ of the GMAW at a heat input of (a) 8.84 kJ/cm and (b) 4.22 kJ/cm.

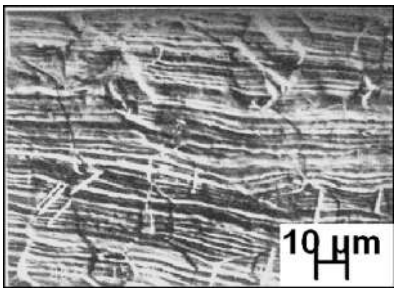

Fig. 11. Typical SEM micrograph showing IGC attack in HAZ of the P-GMAW at a constant heat input of 4.44±0.19 kJ/cm with ϕ=0.41.

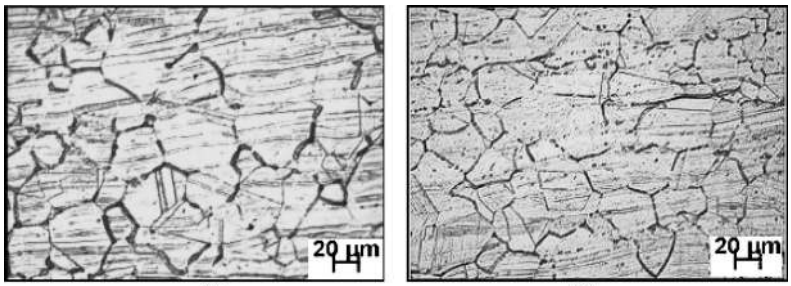

Fig. 12. Typical microphotograph showing IGC attack in HAZ of the P-GMAW at a constant heat input of 4.44±0.19 kJ/cm with (a) ϕ=0.12 and (b) ϕ=0.41.

the more significant corrosion attack on the lined up precipitation of carbides (arrow marked) at the grain boundaries which are more clearly revealed in the micrograph of the GMA weld joint prepared at relatively higher heat input of 8.84 kJ/cm.

In case of using P-GMAW at a given heat input (4.44 kJ/cm) it is found (Table 5) that the increase of ϕ also reduces d by getting it similar to that found in case of GMAW at ϕ of 0.41. However, a comparison of the results presented in Tables 4 and 5 interestingly depict that at a given heat input of similar order (4.22–4.44 kJ/cm), the use of P-GMAW reduces the grain boundary thickening in comparison to that observed in case of GMAW and the increase of ϕ (**Fig. 12**) further reduces the same which may be considered beneficial to the corrosion susceptibility of the weld joint. This may have primarily attributed to the effect of ϕ on temperature of the weld metal deposition that reduces with an increase in it.[8–10] This distance d primarily depends upon weld isotherm and thermal cycle of any location of HAZ leading to significant amount of sensitization in the temperature range of 650–850°C. The variations in welding parameters of GMAW and P-GMAW processes, primarily related to current and voltage, significantly affect the geometries of the arc and weld. Thus, it influences the weld isotherm and thermal cycle of any location of HAZ with respect to its distance from weld centre and consequently affecting the d.

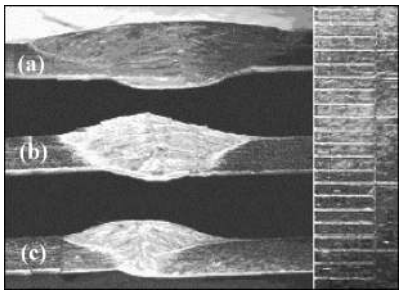

Fig. 13. Typical geometry of the continuous current GMA weld joints at the heat inputs of (a) 8.84 kJ/cm, (b) 6.66 kJ/cm and (c) 4.22 kJ/cm.

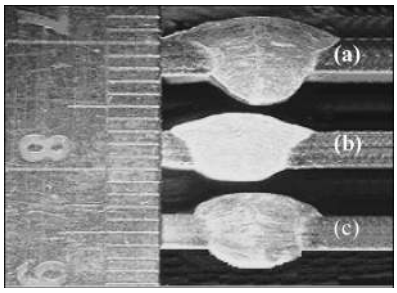

Fig. 14. Typical geometry of the pulsed current GMA weld joints at heat input of 4.44±0.19 kJ/cm by varying the ϕ from (a) 0.12 (b) 0.23 and (c) 0.41.

3.3. Studies on Weld Characteristics

Typical geometry of the GMA weld prepared at different heat input of 8.84, 6.66 and 4.22 kJ/cm, as shown in **Figs. 13**(a)–13(c) respectively, has been given in Table 2. Similarly typical geometry of the P-GMA weld prepared at different ϕ of 0.12, 0.23 and 0.41, as shown in **Figs. 14**(a)–14(c) respectively, has also been given in Table 3, where the heat input has been kept constant of the order of 4.44±0.19 kJ/cm. The Tables 2 and 3 depict that all the weld beads satisfy DIN 8563 class AS standard (Fig. 4), which indicates that thin stainless steel sheets can be effectively welded by GMAW or P-GMAW processes at a low heat input (4.22 kJ/cm) similar to that used in P-GTAW process.[3] However, in case of GMA weld it is observed that at the said low heat input the root penetration (Fig. 13(c)) has been reduced to an extent practically minimum for the requirement of a full penetration sound weld. Thus it possibly indicates as the limiting level of heat input for carrying out GMAW of a 2.5 mm thick stainless steel. Whereas in case of using P-GMAW at a similar order of low heat input (4.22–4.44 kJ/cm) with different ϕ, an appreciable root reinforcement (Fig. 14) has been marked in comparison to that found in GMA weld joints. It is further observed that the increase of ϕ in P-GMAW considerably reduces the root reinforcement of the weld joints primarily due to decrease in temperature of weld metal deposition.[8–10] An appreciable penetration in P-GMA weld at a low heat input of using small I_m is achieved also due to metal transfer primarily at a high I_P causing increased velocity of depositing droplet.[8] These aspects may be considered as a further advantage of P-GMAW over the GMAW to use it for thin sheet welding at extra low heat with appropriate control of ϕ which may be studied further in detail as it is beyond the scope of present investigation.

In GMA weld joints (Fig. 13) along with root reinforcement, the area of weld joint (WJ) has also been found to reduce considerably with the decrease in heat input. However in P-GMA weld joints (Fig. 14) at a given heat input the increase of ϕ up to 0.41 has been found to relatively reduce the area of weld joint. The effect of heat input and variation

of ϕ at a given heat input (4.44 kJ/cm) on the area of weld joint (WJ), area of weld metal deposition (WM) and dilution (D) in case of GMAW and P-GMAW has been shown in **Figs. 15** and **16** respectively. The Fig. 16 shows that in P-GMA weld joint the increase in ϕ at a given heat input (4.44 kJ/cm) reduces WM along with WJ but enhances D significantly. However, in GMA weld joints (Fig. 15) the decrease of heat input up to 6.6 kJ/cm enhances D followed by a reduction in it with the further decrease in heat input to 4.22 kJ/cm while the WM and WJ reduces continuously as it was observed in case of P-GMAW. A comparison of the results presented in Figs. 15 and 16 interestingly depict that at a given heat input of similar order (4.22–4.44 kJ/cm), the use of P-GMAW produces significantly large WJ and WM in comparison to that observed in case of GMAW. This may have primarily attributed to comparatively larger rate of metal deposition[8–10] in P-GMAW than that occurs in GMAW at a given energy input. It may also be considered as an advantage of using pulsed current over the continuous current in sheet metal welding by GMAW process with proper control of pulse parameter with respect to ϕ. According to dilution the chemical composition of the weld with respect to its carbon content has been estimated stochiometrically. The carbon content being the primary criterion affecting the weld properties has been found to be relatively lower than that of base material in both the cases of GMAW and P-GMAW as shown in Tables 2 and 3 respectively. This has primarily happened due to significantly low carbon content of the filler wire as shown in Table 1.

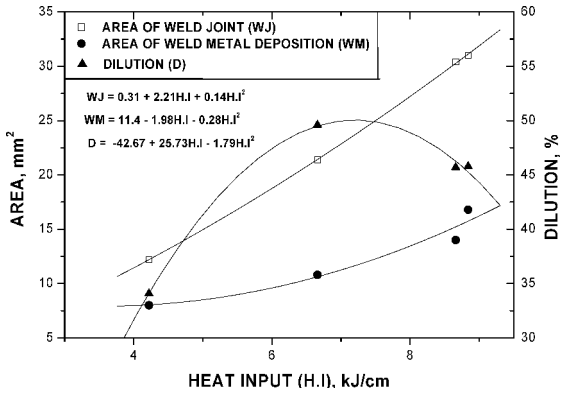

Fig. 15. The effect of heat input on the area of weld metal deposition and its dilution in GMA weld joints.

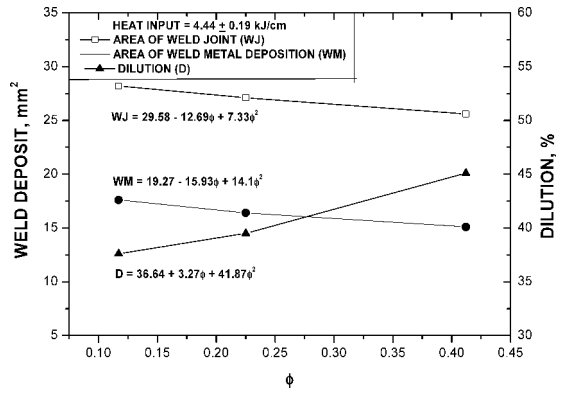

Fig. 16. The effect of heat input on the area of weld metal deposition and its dilution in P-GMA weld joints.

3.4. Microstructure

The weld deposit has been found to have two distinctly different regions of microstructure largely marked as a band of equiaxed cellular dendrite along the region adjacent to the fusion line (FL) and co-axial or columnar dendrite in rest of the matrix. The equiaxed cellular dendritic region adjacent to fusion line primarily resulted from the low degree of constitutional super-cooling[4] in this location of the weld. The width of equiaxed cellular dendritic region observed in the GMA and P-GMA weld joints has been shown in **Tables 6** and **7** respectively. In GMA weld joints it is primarily observed that the width of cellular dendritic region increases with the reduction of heat input indicating higher constitutionally super-cooled zone in the weld adjacent to fusion line. The width of cellular dendritic region observed in GMA weld joints at a heat input of 8.84 and 4.22 kJ/cm have been typically shown in **Figs. 17**(a) and 17(b) respectively. However during P-GMAW it has been interestingly observed that at a similar heat input (4.22–4.44 kJ/cm) as that of GMAW, the increase of ϕ up to 0.41 further enhances the width of cellular dendritic region in the weld metal adjacent to the fusion line.

The typical microphotographs of co-axial dendrite exists

Table 6. Effect of heat input on width of cellular dendrite region in GMA weld joints.

Heat input (kJ/cm)	8.84	8.66	6.66	4.22
Cellular dendrite region width (μm ± σ)	155 ± 15	154 ± 28	209 ± 54	247 ± 94

Table 7. Effect of heat input and ϕ on width of cellular dendrite region in P-GMA weld joints.

Heat input (kJ/cm)	4.44 ± 0.19		
ϕ	0.12	0.23	0.41
Cellular dendrite region width (μm ± σ)	241 ± 26	246 ± 71	264 ± 63

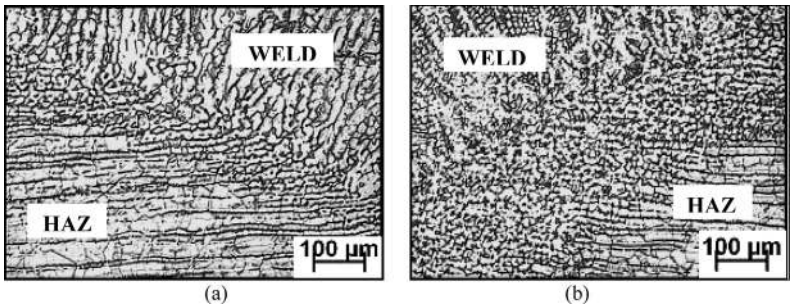

Fig. 17. Typical microphotograph showing the band of cellular zone adjacent to FL of the GMA weld at a heat input of (a) 8.84 kJ/cm and (b) 4.2 kJ/cm.

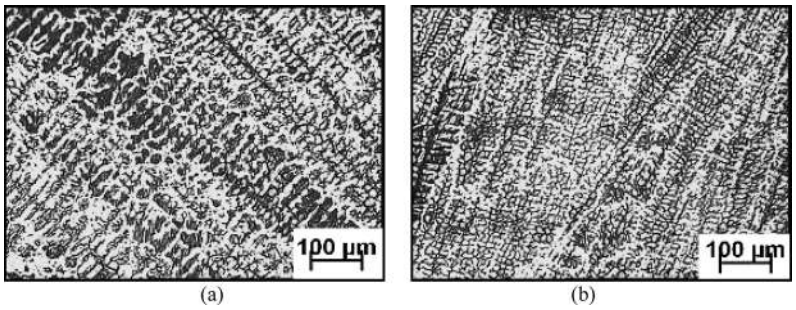

Fig. 18. Typical microphotograph of the GMA weld deposit at a heat input of (a) 8.8 kJ/cm and (b) 4.2 kJ/cm.

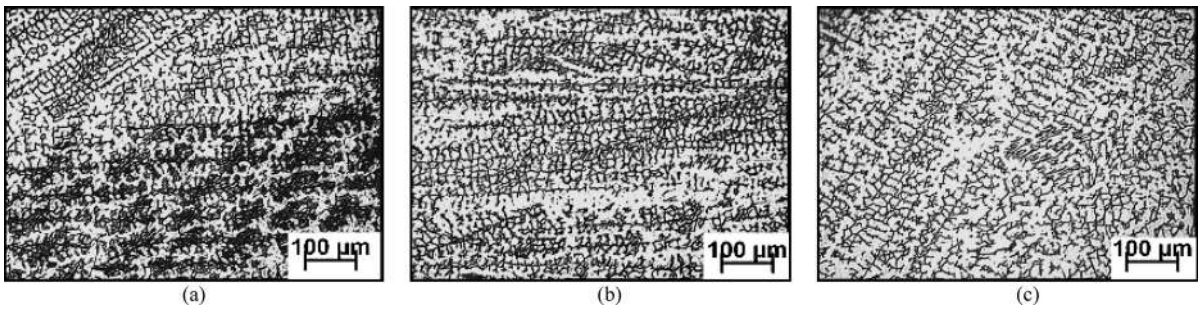

Fig. 19. Typical microphotograph of the P-GMA weld deposit at a constant heat input of 4.44±0.19 kJ/cm with (a) ϕ=0.12 (b) ϕ=0.22 and (c) ϕ=0.41.

in rest of the matrix of weld metal deposited by GMAW at the heat input of 8.84 and 4.22 kJ/cm has been shown in **Figs. 18**(a) and 18(b) respectively. Similarly the typical microphotographs of the co-axial dendrite observed in rest of the matrix of the weld metal deposited by P-GMAW at different f of 0.12, 0.22 and 0.41 has been shown in **Figs. 19**(a)–19(c) respectively where, the heat input was kept constant at 4.44 kJ/cm. In GMA weld deposit a considerable reduction in coarsening of co-axial growth of dendrites has been marked with the lowering of heat input from 8.84 to 4.22 kJ/cm. However in case of P-GMAW the increase in ϕ at a given heat input of 4.44 kJ/cm has been found to considerably reduce the co-axial growth of dendrites in weld deposit along with its refinement (Figs. 19(a)–19(c)) primarily due to lowering of droplet temperature at the time of deposition along with thermal shock introduced by interruption in metal deposition under pulsed current as reported earlier.[8–10] The reduction in co-axial growth of dendrites due to reduction in heat input at GMAW and the increase of ϕ at a given heat input reducing the thermal intensity of weld deposition may have primarily attributed to lowering of degree of constitutional super-cooling.

3.5. Tensile Properties

The ultimate tensile strength, yield strength and elongation of the base material are measured as 658 MPa, 298 MPa and 78% respectively. The effect of heat input on tensile properties of the axial weld joint prepared by GMAW has been shown in **Table 8**. Similarly at a given heat input the effect of ϕ on tensile properties of the axial weld joint prepared by P-GMAW has been shown in **Table 9**. The results presented in Tables 8 and 9 shows that in both the cases of using GMAW and P-GMAW, the weld joint has been found to fracture from weld having comparatively weaker ultimate tensile strength than that of base

Table 8. Tensile properties of GMA weld joints.

Heat Input (kJ/cm)	UTS (MPa)	YS (MPa)	El. (%)	Location of failure
8.84	580	291	44	Weld
8.66	635	309	52	Weld
6.66	530	311	33	Weld
4.22	535	273	36	Weld

Table 9. Tensile properties of P-GMA weld joints.

Heat Input (kJ/cm)	ϕ	UTS (MPa)	YS (MPa)	El. (%)	Location of failure
4.44 ± 0.19	0.12	526	320	36	Weld
	0.23	602	313	54	Weld
	0.41	558	314	42	Weld

metal. However the yield strength and elongation of the welds prepared by both the GMAW and P-GMAW processes are found to be relatively higher and lower respectively than the yield strength and elongation of base material. The comparatively lower elongation of weld is primarily attributed to its cast microstructure, whereas a comparatively lower ultimate tensile strength of the weld was primarily caused by its relatively lower carbon content (Tables 2 and 3) than that of base material. The Table 8 shows that the variation in heat input in the range of 4.22 to 8.84 kJ/cm does not show any significant trend in variation of tensile properties of the weld. At a given heat input, the variation in ϕ (summarized influence of pulse parameters) also has not been found to affect ultimate tensile strength of the weld prepared by P-GMAW process considerably as shown in Table 9. But it may be noted that the tensile properties of the pulsed current gas metal arc welding process is very well comparable to those of the weld prepared by GMAW process. In view of this it may be considered that the use of P-GMAW in welding of thin sheet of S.S is beneficial over the use of GMAW in consideration of favourable influence of P-GMAW especially on intergranular corrosion

susceptibility of heat affected zone, and the other characteristics of weld joint as discussed above.

4. Conclusion

(1) Thin 2.5 mm thick stainless steel sheets can be effectively welded by GMAW or P-GMAW processes at a low heat input of the order of 4.22 kJ/cm, similar to that used in P-GTAW process by other research workers.

(2) The increase of ϕ in P-GMAW considerably reduces the root reinforcement of the weld joints primarily due to decrease in temperature of weld metal deposition and reduction in velocity of depositing droplet.

(3) The use of P-GMAW provides comparatively better resistance to inter granular corrosion along with higher mechanical properties in comparison to those of the conventional GMA weld primarily due to superior control of weld thermal behaviour at relatively lower heat input by suitable control of pulse parameters with respect to their summarized influence defined by a dimensionless factor ϕ.

(4) In comparison to GMAW, the P-GMAW process is more effective in producing relatively finer dendrite in the weld deposit.

Acknowledgement

The authors thankfully acknowledge the financial support provided by the DST-BMBF collaborative programme with TU Berlin to carry out this work at IIT Roorkee.

REFERENCES

1) M. Suban and J. Tusek: *J. Mater. Process. Technol.*, **119** (2001), 185.
2) M. Ushio and C. S. Wu: *Metall. Mater. Trans. B*, **28B** (1997), No. 3, 509.
3) G. Lothangkum, P. Chaumbai and P. Bhandhubanyong; *J. Mater. Process. Technol.*, **89–90**, (1999), 410.
4) E. Folkhard: Welding Metallurgy of Stainless Steels, Springer-Verlag Wien, New York, (1988), 105.
5) S. K. Choi, C. D. Yoo and Y.-S. Kim: *J. Phys. D, Appl. Phys.*, **31**, (1998), 207.
6) H. S. Randhawa, P. K. Ghosh and S. R. Gupta: *ISIJ Int.*, **38** (1998), 276.
7) S. Ueguri, K. Hara and H. Komura: *Weld. J.*, **64** (1985), No. 8, 242s.
8) H. S. Randhawa, P. K. Ghosh and S. R. Gupta: *ISIJ Int.*, **40** (2000), 71.
9) P. K. Ghosh, S. R. Gupta and H. S. Randhawa: *Metall. Mater. Trans. A*, **31A** (2000), No. 9, 2247.
10) P. K. Ghosh, V. K. Goyal, H. K. Dhiman and M. Kumar: *Sci. Technol. Weld. Joining*, **11** (2006), No. 2, 232.
11) ASM Handbook-Welding, Brazing and Soldering, ASM Int. Handbook Committee, Materials Park, OH, USA, 6, (1993), 33.
12) S. Kulkarni, P. K. Ghosh, S. Ray, H. S. Kushwaha, K. K. Vaze, P. K. Singh and J. Krishnan: Proc. of the IIW-IC-2005, IIW, Mumbai, (2005), 43.
13) P. K. Ghosh, S. R. Gupta and H. S. Randhawa: *Int. J. Joining Mater.*, **12** (2000), No. 3, 76.